Fish Cage Waste Dispersal in Jordan Bay

Adam Drozdowski, Brent Law and Fred Page

Coastal Ecosystem Sciences Division
Maritimes Region
Fisheries and Oceans Canada

Bedford Institute of Oceanography
P.O. Box 1006
Dartmouth, Nova Scotia
Canada B2Y 4A2

2018

Canadian Technical Report of Fisheries and Aquatic Sciences 3269

Fisheries and Oceans Canada | Pêches et Océans Canada

Canada

Canadian Technical Report of Fisheries and Aquatic Sciences

Technical reports contain scientific and technical information that contributes to existing knowledge but which is not normally appropriate for primary literature. Technical reports are directed primarily toward a worldwide audience and have an international distribution. No restriction is placed on subject matter and the series reflects the broad interests and policies of the Department of Fisheries and Oceans, namely, fisheries and aquatic sciences.

Technical reports may be cited as full publications. The correct citation appears above the abstract of each report. Each report is abstracted in Aquatic Sciences and Fisheries Abstracts and indexed in the Department's annual index to scientific and technical publications.

Numbers 1 - 456 in this series were issued as Technical Reports of the Fisheries Research Board of Canada. Numbers 457 - 714 were issued as Department of the Environment, Fisheries and Marine Service Technical Reports. The current series name was changed with report number 925.

Technical reports are produced regionally but are numbered nationally. Requests for individual reports will be filled by the issuing establishment listed on the front cover and title page. Out-of-stock reports will be supplied for a fee by commercial agents.

Rapport technique canadien des sciences halieutiques et aquatiques

Les rapports techniques contiennent des renseignements scientifiques et techniques qui constituent une contribution aux connaissances actuelles, mais que ne sont pas normalement appropriés pour la publication dans un journal scientifique. Les rapports techniques sont destinés essentiellement à un public international et ils sont distribués à cet échelon. Il n'y a aucune restriction quant au sujet; de fait, la série reflète la vaste gamme des intérêts et des politiques du ministère des Pêches et des Océans, c'est-à-dire les scences halieutiques et aquatiques.

Les rapports techniques peuvent être cités comme des publications complètes. Le titre exact paraît au-dessus du résumé de chaque rapport. Les rapports techniques sont résumés dans la revue Résumés des sciences aquatiques et halieutiques, et ils sont classés dans l'index annual des publications scientifiques et techniques du Ministère.

Les numéros 1 à 456 de cette série ont été publiés à titre de rapports techniques de l'Office des recherches sur les pêcheries du Canada. Les numéros 457 à 714 sont parus à titre de rapports techniques de la Direction générale de la recherche et du développement, Service des pêches et de la mer, ministère de l'Environnement. Les numéros 715 à 924 ont été publiés à titre de rapports techniques du Service des pêches et de la mer, ministère des Pêches et de l'Environnement. Le nom actuel de la série a été établi lors de la parution du numéro 925.

Les rapports techniques sont produits à l'échelon regional, mais numérotés à l'échelon national. Les demandes de rapports seront satisfaites par l'établissement auteur dont le nom figure sur la couverture et la page du titre. Les rapports épuisés seront fournis contre rétribution par des agents commerciaux.

Canadian Technical Report of
Fisheries and Aquatic Sciences 3269

2018

Fish Cage Waste Dispersal in Jordan Bay

by

Adam Drozdowski, Brent Law and Fred Page

Science Branch
Maritimes Region
Fisheries and Oceans Canada

Bedford Institute of Oceanography
P. O. Box 1006
Dartmouth, Nova Scotia
Canada B2Y 4A2

© Her Majesty the Queen in Right of Canada, 2018.
Cat. No. Fs 97-6/3269E-PDF ISBN 978-0-660-27317-4 ISSN1488-5379

Correct Citation for this publication:

Drozdowski, A., B. Law and F. Page. 2018. Fish Cage Waste Dispersal in Jordan Bay. Can. Tech. Rep. Fish. Aquat. Sci. 3269: viii + 35p.

TABLE OF CONTENTS

SCIENCE BRANCH I

BEDFORD INSTITUTE OF OCEANOGRAPHY I

LIST OF FIGURES IV

LIST OF TABLES IV

ABSTRACT V

RÉSUMÉ VI

INTRODUCTION 1

2: MODEL FORCING AND SETUP 2

2.1 CURRENTS 5

2.2 WAVES 7

2.3 FRICTION VELOCITIES 8

2.4 DESCRIBING THE BOTTOM VELOCITY PROFILE 11

2.5 SIMULATIONS SETUP 17

3: RESULTS 20

3.1 FULL FORCING SIMULATION 20

3.2 ALTERNATIVE FORCING SIMULATIONS 24

4: DISCUSSION 29

ACKNOWLEDGMENTS 34

REFERENCES 34

LIST OF FIGURES

Figure 1 Red circle shows locations of the 2014 current meter deployments....3
Figure 2 Segment of ADCP 67_1 profile. Color scale is centimeters per sec. north....7
Figure 3 Significant wave height, period and direction. Recorded by 67_1....8
Figure 4 Currents and wave friction velocity....9
Figure 5 Currents only friction velocity....10
Figure 6 Scatter plots of currents and waves (left) and currents only (right) friction velocities....11
Figure 7 North component of velocity from RDI's 66_1 and 67_1....13
Figure 8 Regression analysis between north component of velocity from RDI's 66_1 and 67_1....13
Figure 9 Aquadopp east (top) and north (bottom) velocity profile....14
Figure 10 Aquadopp east (top) and north (bottom) velocity profile(Part 2)....15
Figure 11 Speeds at 1 mab....16
Figure 12 Root mean square velocity profile....16
Figure 13 Normalized bottom concentration under fish cage for the 4 sediment classes forced with the Full forcing scenario....21
Figure 14 Normalized concentration 1 meter above bottom under fish cage for the 4 sediment classes forced with the Full forcing scenario....22
Figure 15 Near field and far field normalized mean bottom concentration for 4 waste class scenarios for the Full forcing simulation....23
Figure 16 Normalized bottom concentration under fish cage for the 4 sediment classes forced with the Log-layer forcing scenario....25
Figure 17 Near field and far field normalized mean bottom concentration for 4 waste class scenarios for the Log-layer forcing simulation....26
Figure 18 Normalized bottom concentration under fish cage for the 4 sediment classes forced with the Lin-layer forcing scenario....27
Figure 19 Near field and far field normalized mean bottom concentration for 4 waste class scenarios for the Lin-layer forcing simulation....28
Figure 20 Normalized bottom concentration under fish cage forced with the Full scenario for feed pellets....32
Figure 21 Near field and far field normalized mean bottom concentration for 4 waste class scenarios for the Full forcing simulation (base 10 logarithmic color scale)....33

LIST OF TABLES

Table 1 Current Meter Deployment details....4
Table 2 Statistical summary of the current meter data sets....6
Table 3 Forcing scenarios used in simulations....17
Table 4 Waste Class Parameters used in simulations....18
Table 5 BBLT Simulation Parameters....19
Table 6 Summary of Results....29

ABSTRACT

Drozdowski, A., B. Law and F. Page. 2018. Fish Cage Waste Dispersal in Jordan Bay. Can. Tech. Rep. Fish. Aquat. Sci. 3269: viii + 35p.

Waste dispersal from a fin-fish aquaculture facility in Jordan Bay N.S. was simulated using the benthic boundary layer transport model (BBLT). The currents, waves and bottom stress were measured during the fall of 2014 and used as inputs. Four waste classes were considered: fines, flocs, fecal waste and feed pellets, and modelled with a 46 day continuous release scenario. The resulting concentration varied by as much as 6 orders of magnitude. The four classes peaked at 0.003, 0.082, 122.4 and 234.6 g/m^3 inside the cage. Spatial patterns reveal the concentration of the fines to be relatively uniform inside and within a few hundred meters of the cage, and to fall by 1/10 a few kilometers away. Floc concentrations fall to 1/10 within a 100 m of the cage and by 1/1000 within a few kilometers. The higher concentrations of fines and flocs in far field, as compared to fecal material and pellets, represent a transport mechanism for constituents such as trace metals, pesticides and organics which have an affinity for large surface area fine-grain sediments.

For fecal waste, concentrations fall by 1/10 directly outside the cage and should be undetectable a kilometer away. Feed Pellet removal is somewhat more complicated due to the episodic deposition and advection of the sediment patch. However, just like for the fecal waste the concentration drops by at least an order of magnitude directly outside the cage and by as much as 1/1000 within a few hundred meters. The general direction of travel is to the south. Overall the concentrations (particularly for the heavier waste) were found be very sensitive to the choice of bottom parameterization and require tuning and validation with field data before the model can be used to accurately predict concentrations.

Alternative forcing scenarios were used to investigate the relative importance of wave induced bottom stress and near bottom currents. These scenarios ignored observations in 5m near the bottom and instead extrapolated the currents using a (i) logarithmic, and (ii) linear near bottom profile and derived the bottom stress from a quadratic drag law. The outcome was higher concentrations. For fines and flocs the difference is about 2 orders of magnitude and attributed to episodic deposition which occurs in the absence of wave induced bottom stress. For the fecal and feed waste, there is also more deposition but the choice of linear vs logarithmic bottom profile is the critical factor with the linear scenarios accumulating waste over the whole simulation while the logarithmic showing more resemblance to the realistic scenario. Evidently what matters for the heavier waste classes, is the forcing in the 10 cm near the bottom where this waste resides. This comparison underlines the importance of accurate near-bottom currents and bottom stress in modelling efforts.

RÉSUMÉ

Drozdowski, A., B. Law and F. Page. 2018. Dispersion des déchets des cages à poisson à Jordan Bay. Can. Tech. Rep. Fish. Aquat. Sci. 3269: viii + 35p.

La dispersion des déchets provenant d'une installation d'aquaculture de poissons à nageoires située à Jordan Bay (Nouvelle-Écosse) a été simulée à l'aide du modèle de transport dans la couche limite de la zone benthique. Les courants, les vagues et les facteurs de stress en fond marin ont été mesurés au cours de l'automne 2014 et utilisés comme intrants. Quatre catégories de déchets ont été déterminées : les fines, le floc, les déchets fécaux et les pelotes. Elles ont été modélisées dans un scénario de rejet continu de 46 jours. Les concentrations obtenues étaient caractérisées par une variation allant jusqu'à six ordres de grandeur. Les quatre classes ont culminé à 0,003 g/m^3, à 0,082 g/m^3, à 122,4 g/m^3 et à 234,6 g/m^3 à l'intérieur de la cage. Les tendances spatiales ont révélé que la concentration des fines est relativement uniforme à l'intérieur de la cage et à quelques centaines de mètres autour de celle-ci, et qu'elle diminue d'un dixième quelques kilomètres plus loin. Les concentrations de floc diminuent d'un dixième dans une zone de 100 mètres autour de la cage et d'un millième dans une zone de quelques kilomètres. Les concentrations élevées de fines et de floc situées loin de la cage, comparativement à celles des déchets fécaux et des pelotes, représentent un mécanisme de transport pour les composantes comme les métaux à l'état de traces, les pesticides et les matières organiques qui ont une affinité pour les sédiments à grain fin à grande surface.

Pour ce qui est des déchets fécaux, les concentrations diminuent d'un dixième directement à l'extérieur de la cage et devraient être indétectables à une distance d'un kilomètre de celle-ci. Le retrait des pelotes est un peu plus compliqué en raison du dépôt épisodique et de l'advection des zones sédimentaires. Cependant, tout comme pour les déchets fécaux, la concentration diminue d'au moins un ordre de grandeur directement à l'extérieur de la cage et d'un millième à quelques centaines de mètres de celle-ci. La direction de déplacement est généralement orientée vers le sud. Dans l'ensemble, les concentrations (en particulier celles des déchets lourds) étaient très sensibles au paramétrage du fond; elles nécessitent un réglage et une validation à l'aide des données recueillies sur le terrain avant que le modèle puisse être utilisé pour prévoir les concentrations avec exactitude.

D'autres scénarios de forçage ont été utilisés pour étudier l'importance relative des facteurs de stress en fond marin provoqué par les vagues et des courants proches du fond. Ces scénarios ne tenaient pas compte des observations effectuées à cinq mètres du fond et ont plutôt extrapolé les courants à l'aide d'un profil de fond (i) logarithmique et (ii) linéaire, et ont dérivé les facteurs de stress en fond marin selon une loi de traînée quadratique. Le résultat obtenu était des concentrations plus élevées. Pour les fines et le floc, la différence est d'environ deux ordres de grandeur, et elle est attribuable au dépôt épisodique qui se produit en l'absence de facteurs de stress en fond marin provoqué par les vagues. Pour ce qui est des déchets fécaux et des pelotes, il y a également une hausse des dépôts. Cependant, le choix de profil de fond, c'est-à-dire linéaire ou logarithmique, est le facteur le plus important. Dans les scénarios linéaires, les déchets sont accumulés pendant l'ensemble de la simulation, tandis que les scénarios logarithmiques présentent une plus grande ressemblance avec le scénario réaliste. De toute évidence, le plus important pour les classes de

déchets lourds est le forçage dans les dix centimètres les plus près du fond, là où ces déchets se trouvent. Cette comparaison souligne l'importance de l'exactitude des efforts de modélisation des courants proches du fond et des facteurs de stress en fond marin.

INTRODUCTION

Fin fish aquaculture in marine coastal waters is a growing industry worldwide as well as in Atlantic Canada. Farmed fish are typically cultivated in circular cages suspended in the upper layer of the water column. The fish are nourished by feed pellets. Any uneaten pellets, as well the fecal waste, are deposited into the benthic environment generally beneath the cage. The removal of this waste is dependent on physical advection and dispersion processes. The modelling of these processes can aid operators and regulators in determining environmental impacts and optimal carrying capacities.

This report describes the use of current meter, waves and bottom stress data collected during the September 2014, to simulate waste dispersal from an active aquaculture facility in Jordan Bay. The modelling was completed using the benthic boundary layer transport model (BBLT), which was originally developed and used to study suspended particulate drilling waste (Hannah et al., 1995). Sediment dynamics are modelled with a modified Rouse profile (Rouse 1937). Basic output from this numerical model consists of drift, diffusivity, and concentration. Inputs are time series of the current profile, bottom stress and settling velocity. The most recent version of the model (version 7; Drozdowski et al., 2004) includes a wave boundary layer based on Grant and Madsen (1986) and Li and Amos (2001), bottom stress dependent floc breakup and growth-days-lost benthic biological impacts based on Cranford et al., (2003).

Past applications of BBLT were mostly in the offshore environment (Hannah and Drozdowski, 2005; Tedford et al., 2003, 2002), where the fate and sub-lethal biological impacts of drilling mud released during the drilling phase of oil and gas platforms, such as Hibernia on the Grand Banks and North Triumph on the Scotian Shelf, was of primary concern.

Some near-shore work was undertaken using BBLT as well. AMEC E&E division has used BBLT to conduct an environment assessment of the discharge of effluent solid waste in Long Harbour (AMEC E&E Division, 2007) and the construction activities associated with the Strait of Belle Isle submarine cable crossings (AMEC E&E Division, 2011). Moreover, Petrie et al. (2004) have used BBLT in a study of Sydney Harbour and found a tendency to accumulate sediment near the head of the harbour which is fairly consistent with the distribution of pollutants found in the sediment.

The applicability of BBLT to the near-shore is limited by spatial variability of the current which in the presence of topographic features can vary significantly in magnitude and direction over 100's of meters. Attempts to overcome spatial variability have resulted in BBLT3D which works under the same principles but uses 3 dimensional current fields produced by circulation models (Drozdowski, 2009). This method is more computationally demanding and is often limited by the availability of reliable, validated and adequately resolved circulation models.

Niu et al. (2014) has performed a case study to compare BBLT with another sediment transport model, ParTrack (Rye et al., 1998). Although ParTrack and BBLT are formulated quite differently, the case study shows comparable results, especially for locations several kilometers away from the discharge.

This report is laid out as follows. Section 1 offers a description of model forcing (e.g. currents and waves), model setup and details of the simulation. Also presented, is a description of the analysis on the forcing required to convert it to a form required for BBLT. Chapter 3 describes the results of the model runs while Chapter 4 discusses the model results in more depth and offers broader interpretation and conclusion.

2: MODEL FORCING AND SETUP

BBLT was forced with time series of the profile of currents and bottom stress. The required data was collected in the fall of 2014 using 3 acoustic doppler current meters (ADCP) moored near bottom in close proximity of a fin-fish aquaculture facility in Jordan Bay (Figure 1, Table 1). ADCP 67_1 faced upward to measure currents and waves while 66_1 pinged downward at a higher ping rate in order to resolve near bottom flow. ADCP 66_1 deployment only lasted 2 days while 1 provided 70 days of data. For further deployment and QC details refer to Page et al. (2016). The aquadopp profiler sampled currents at a very high ping rate in the bottom meter of the water column. The high sampling rate provided currents as well as currents and wave induced bottom stress. The aquadopp deployment lasted 46 days. Overall bin correlations were high at 88% mean and 12% standard deviation for the 14 top bins used for the modelling. The quality in the lowest 3 bins degraded and they were excluded. This section presents a brief summary of the data collected from the 3 instruments as well BBLT model setup details.

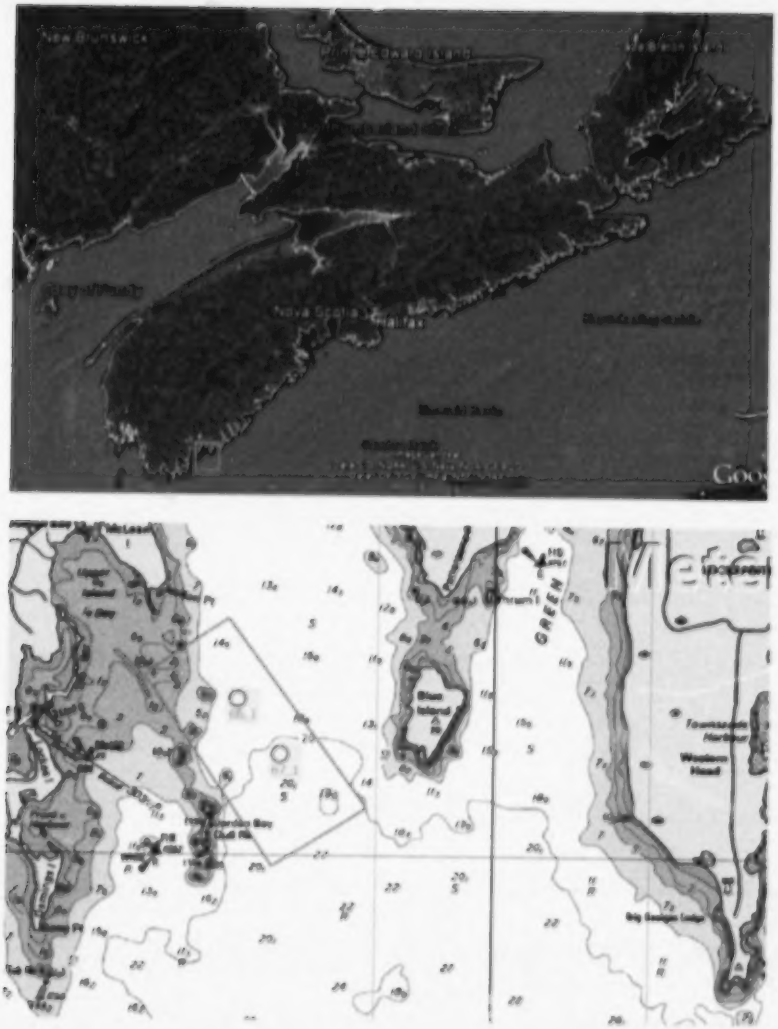

Figure 1 Red circle shows locations of the 2014 current meter deployments. Red outline shows the location of the aquaculture facility.

Table 1 Current Meter Deployment details. Depth refers to mean depth of instrument as indicated by the pressure sensor and mooring configuration. mab=meters above bottom.

Short-hand Name used in report	Model	Longitude (°W)	Latitude (°N)	Orientation	Waves	Number of bins / size (m)	Depth (m)	mab(1st bin)	Start time	End time	Sampling Period	Number of Pings /duration (min)
67_1	RDI Workhorse 600 KHz	65.1994	43.6781	up	Yes	18/1	22.8	4.7	24/09/2014 13:18	04/12/2014 17:33	20 min	60/5
66_1	RDI Workhorse 1200 KHz	65.2062	43.6842	down	No	31/0.1	18.3	3	23/09/2014 12:39	25/09/2014 14:49	10 min	60/5
aquadopp	Nortek Aquadopp; 2 MHz	65.2062	43.6842	Side-looking	Yes	17/0.08	18.1	1.1m	23/09/2014 06:00	12/11/2014 18:02	2 h	2400/5

2.1 CURRENTS

Current data from the 3 instruments is summarized in Table 2 for selected depths. Maximum speeds generally don't exceed 30 cm/s. The root mean square (rms) speeds at 5 mab (meters above bottom) is the highest. The highest speeds would typically be near the surface but as the ADCP does not resolve the top 10% of the water column (Teledyne RD Instruments, 2014) due to surface reflection, we are missing the peak of the Ekman drift in the data, but capturing the return bottom flow. The rms falls off sharply near the bottom as indicated by the aquadopp, reaching 1 cm/s at 0.1 mab. The principle axis (axis of maximum variance) is north-south (along the bay axis) with a ratio 2:1 between major and maximum axis.

Tidal analysis of 67_1 indicates that tides account for about 25-40% of total variance. Diurnal tide M2 dominates tidal flow at around 80% of total tidal energy and just as the principle axis is directed along the bay with a ratio of 7:1 between major and minor components. Data from 66_1 was too short for tidal analysis. The aquadopp shows decreasing tidal presence to the point of being unresolvable in the bottom bin. There is a near-bottom rotation towards northwest of the major axis (consistent with the principle axis). Such a counter-clockwise rotation in the bottom layer is consistent with bottom drag induced Ekman spiral.

Figure 2 shows a segment of the profile of the northward (into the bay) current from 67_1. Semi-diurnal tides have a visible underlying presence but there is also at 2-layer flow structure (e.g days 310.8-312) which has near bottom amplification into the bay compensated by increased outflow near the surface. This kind of current structure is characteristic of surface Ekman drift and bottom adjustment drift caused by alongshore wind (Csanady 1982; see Fig 2.14).

Table 2 Statistical summary of the current meter data sets. All speeds in cm/s. P-ax = principle axis (or axis of maximum variance).

	ADCP 67_1			ADCP 66_1		Aquadopp	
Bin # (mab)	**1 (5)**	**7 (11)**	**14(18)**	**3(0.3)**	**25(2.5)**	**1(1.06)**	**7(0.1)**
Mean u	0.31	0.92	0.02	-0.17	0.35	-0.74	-0.09
Mean v	-0.6	2.5	0.59	-0.36	-1.26	0.64	0.23
Max. speed	28.53	31.06	30.51	11.29	18.12	12.38	3.87
Min. speed	0.14	0.11	0.14	0.4	0.09	0.02	0.01
RMS speed	11.1	9.3	8.5	5.3	7.2	3.9	1.05
P-ax. (deg. T)	-0.1	-1.2	-2.9	-11.8	-8.2	-53.0	-13.1
P-ax. major speed	10.1	8.1	7.4	4.9	6.7	3.2	0.8
P-ax. minor speed	4.5	3.6	4.2	3.1	3.1	1.5	0.6
M2 maj.	7.0	7.4	6.6	—	—	1.9	—
M2 min.	-0.9	-1.1	-1.1	—	—	-0.5	—
M2 inc. (deg. T)	-4.3	-6.4	-9.3	—	—	-55.7	—
M2 pha. (GMT)	283.7	288.2	285.2	—	—	339.8	—
Tide as % of Tot. Var.	24.7	42.1	38.8	—	—	22.1	—
M2 as % of Tot. Tide	81.0	83.8	78.8	—	—	69.5	—
Sample Count	5125	5125	5125	302	302	606	606

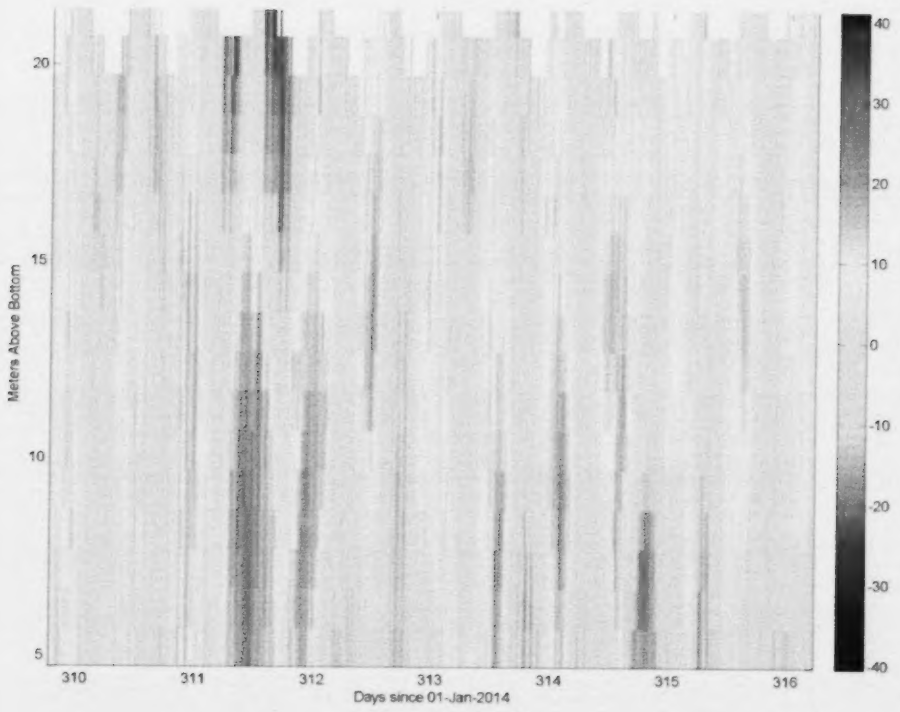

Figure 2 Segment of ADCP 67_1 profile. Color scale is centimeters per sec. north.

2.2 WAVES

Wave observations from 67_1 are presented in Figure 3. Significant wave heights reached 3 m during the sampling period. Wave periods were in the range of 5 to 15 seconds while direction generally from the southeast to southwest, with the biggest waves out of southwest. Large wave events can re-suspend and redistribute the sediment. BBLT accounts for wave action by its contribution to bottom stress and currents.

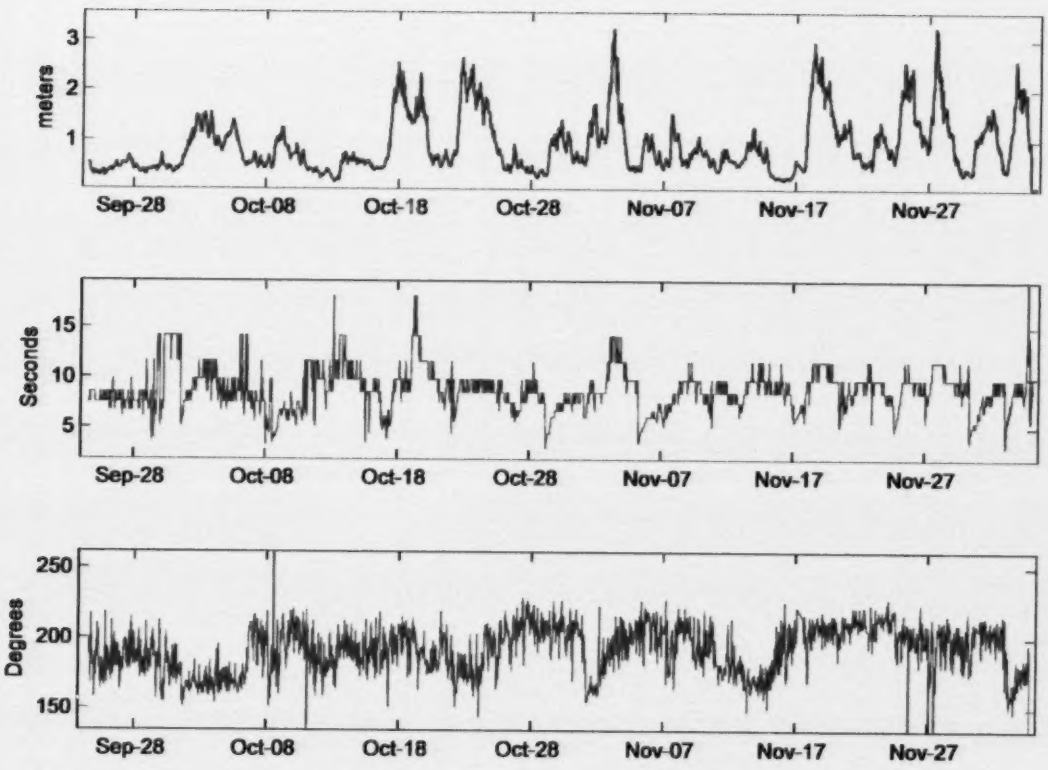

Figure 3 Significant wave height (top), period (middle) and direction (bottom) from which waves are travelling (Deg. True). Recorded by 67_1.

2.3 FRICTION VELOCITIES

Bottom stress (or friction velocity; will be used interchangeable here) determines re-suspension rates in BBLT and hence is one of the most critical parameters. Higher friction velocities will bring more of the sediment higher up in the water column exposing it to stronger currents and hence more transport. Friction velocity is caused by bottom currents as well as waves provided they are large enough compared to the depth for wave orbital velocities to penetrate to the bottom. The aquadopp measured the currents friction velocity as well as the combined waves and currents friction velocity. A third parameter is the bottom boundary layer height (not shown), a parameter typically under a few centimeters but in the presence of large waves as large as 5-10 cm. These 3 parameters are required by BBLT to run in the wave boundary layer mode. This full waves run will be used for the main results here. BBLT can also run in a currents only bottom stress mode where the friction velocity is computed from the current time series nearest to the bottom (5 mab) using a quadratic drag law (drag coefficient C_d=0.005. This choice of drag was used for consistency with older applications of BBLT (e.g. Tedford et al., 2003). It is referenced to 1 mab and the currents are extrapolated down to 1 mab using

a log-layer profile. This configuration was applied to alternative forcing scenarios for purpose of understanding the relative importance of wave contributions.

To validate the aquadopp bottom stress data, the wave induced bottom stress was also computed directly from the 67_1 data using the sediment transport model SEDTRANS96 (Li and Amos, 2001). The deepest bin (5m) of 67_1 was used in the calculation along with the wave height, period and direction.

Figure 4 shows combined wave and current friction velocity from the aquadopp and computed with SEDTRANS96. Values usually exceed 0.01 m/s and can reach 0.05. The large wave events clearly correspond to large wave heights (overlaid in the Figure 4 for clarity). Six such events (or storms) are noted, E1=Oct 2-5, E2=Oct 17-20, E3= Oct 22-24 and E4=Nov 3, E5=Nov 20 and E6=Nov 25-27, along with several smaller events as well as general increase in wave activity (trend) during the period. The currents only friction velocities from the aquadopp, computed by SEDTRANS96 and the drag law are shown in Figure 5.

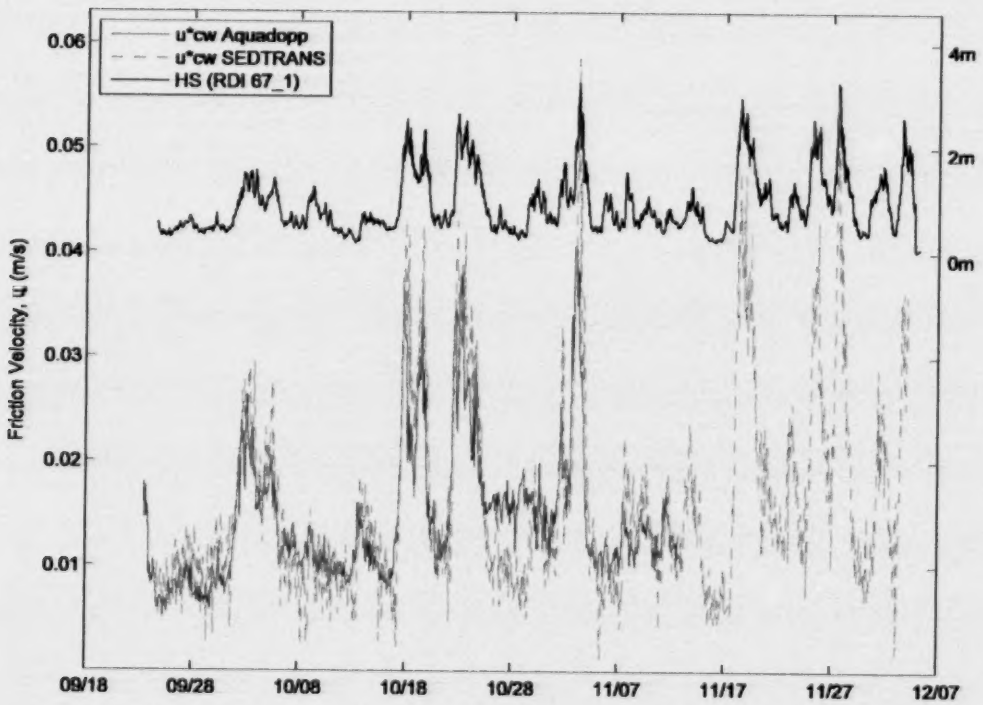

Figure 4 Currents and wave friction velocity measured by aquadopp and calculated by SEDTRANS. Observed significant wave height overlaid to show wave events (scale on the right).

The agreement between the aquadopp wave and currents stress and the SEDTRANS96 is excellent. This can be seen in the time series as well in a scatter plot (Figure 6) which gives an R^2 of 0.73. SEDTRANS96 tends to gives slightly higher values for large wave events and lower values for some of the small wave states. The disagreement at low wave states is expected as SEDTRANS96 does not have access to the correct bottom currents. For the currents only stress, the agreement between SEDTRANS96 and aquadopp is poor. SEDTRANS does agree much better with the drag law as expected, as these two estimates do not capture the full effect of wave induced bottom currents. Nonetheless, all 3 are in the range 0-0.02 m/s.

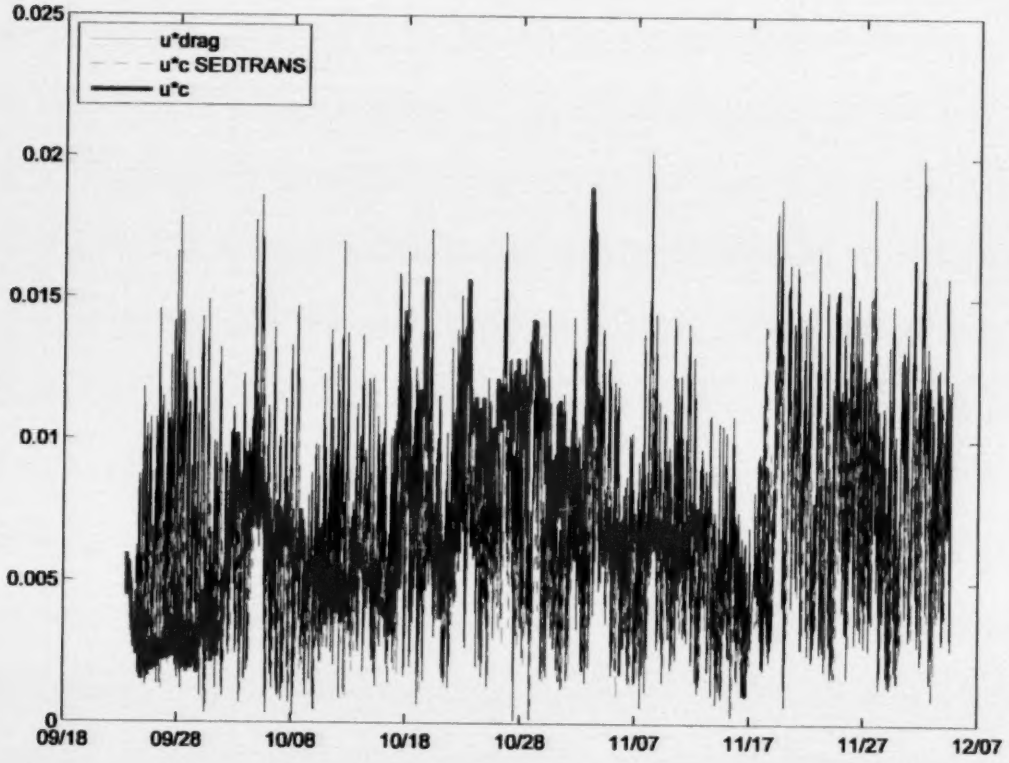

Figure 5 Currents only friction velocity. From the top in legend: drag law estimated, SEDTRANS96 derived and measured by aquadopp.

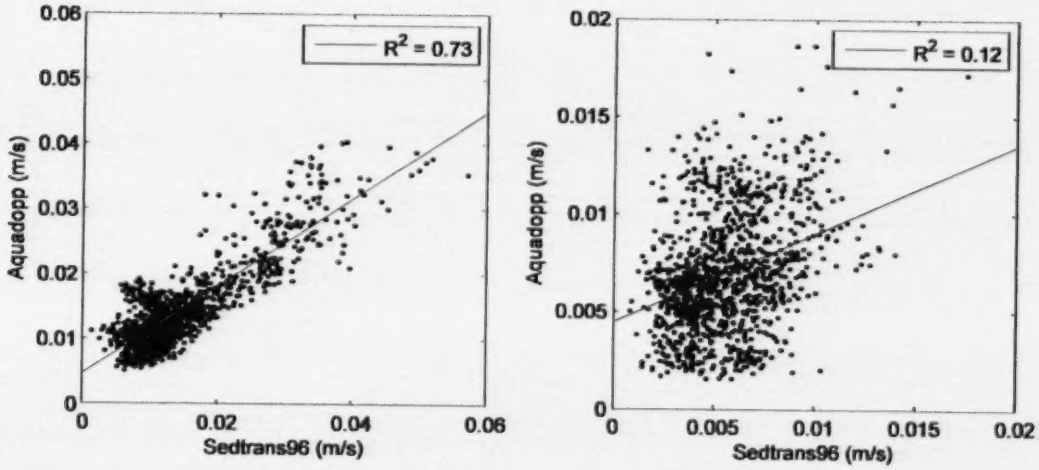

Figure 6 Scatter plots of currents and waves (left) and currents only (right) friction velocities. Blue line shows linear regression fit.

2.4 DESCRIBING THE BOTTOM VELOCITY PROFILE

Sediment dynamics are highly sensitive to near bottom currents and bottom stress. This is particularly the case for heavier particles which are near the bottom most of the time and the primary reason for the deployment of the aquadopp and the downward facing RDI's. The time series from 66_1 was too short to be used as BBLT input, but was found to correlate well with 66_1. Figure 7 shows the overlap for the north velocity component. This suggest the possibility of using the long 67_1 time series to calculate currents closer to the bottom using a derived relationship between 67_1 and 2. These currents would then be used as BBLT input. Figure 8 shows the scatter plot of the north current in bottom bin of 67_1 and average of bins 21 to 31 from 66_1 (this series was averaged to reduce noise). The scatter plot shows a strong linear trend. Linear regression coefficients were used to generate north currents at 1.5 and 2.5 mab based on the 4.7 mab 67_1 currents. The quality of fit, R^2 is 0.66 for the 2.5 mab fit and 0.61 for 1.5 mab.

The east components of the 2 current meters were uncorrelated ($R^2 < 0.1$) while the east component of 66_1 had a slight negative correlation with north component of 67_1 (R^2~-0.3). Hence the approach taken for the north component was not applicable, instead the east component was supplied stochastically by taking the short east 66_1 time series as cyclically repeating.

A long time series of bottom current data was available from the aquadopp. An energetic fragment from around storm E1 of the profile time series is shown in Figure 9. Although the tides are generally weak (~1 cm/s; see Table 2) this fragment shows a burst of tidal energy peaking at ~7 cm/s. There appears to be a transition layer between the water column velocity profile and the bottom boundary layer at around 0.5 m where the velocity rapidly decreases to near zero. Another fragment is shown in Figure 10. Here, the layer transition is once again at 0.5 mab but the bottom layer has current in the opposite direction to the top. It's likely that the aquadopp, which is sampling at a rapid

rate, is capturing the turbulent bottom boundary layer which episodically transitions between a turbulent and laminar flow states. Typically, past modelling efforts have assumed a smooth (laminar) log layer profile below 1m. The effect of this type of structure in the bottom 1m of water will be investigated here.

A puzzling feature of the aquadopp current data is its lack of correlation with data from the other instruments. The correlation of the aquadopp time series with 66_1 at same depth is 0.2. The 1 mab speeds are plotted for in Figure 11. ADCP 66_1 speeds were higher and more variable. There are 2 possible explanations; (1) the ping rate of 66_1 is inadequate to resolve the turbulent near bottom flows; (2) the locations of the 2 instruments are too far apart to correlate small scale turbulence features.

The whole current profile from the aquadopp was used for BBLT simulations (some vertical averaging of bins was used to reduce noise). The lowest level was 0.1 mab. BBLT used a log layer to generate currents below this (For details see Drozdowski 2004).

If the aquadopp and 66_1 data were not available, the standard approach would be to fit a log layer (or linear) profile based on the currents nearest to the bottom (4.7 mab here). Figure 12 shows the vertical profiles of rms speeds computed from a log layer and linear fit along with the actual vertical profile of the rms speeds. The method clearly overestimates the near bottom currents, in some cases quite severely (e.g. at 0.5 mab the log layer gives 7cm/s while it's actually only 1cm/s !). A linear profile seems more appropriate but this leads to very small speeds very close to the bottom (notice aquadopp speeds level of to 1cm/s below 0.5 mab). The outcomes of these 2 extrapolation methods will be investigated with alternative BBLT forcing scenarios. A better fit to the bottom profile can also be obtained if a different value is used for the roughness height. However, to see improvement, roughness height would have to be increased by a factor of a hundred and considered unphysical based on grain size constraints discussed below. Another approach worth investigating but is beyond the scope of the present work is to use the bottom current profile which can be extracted from SEDTRANS96. This model uses wave information to generate a more realistic bottom profile than can be obtained by extrapolating the currents alone.

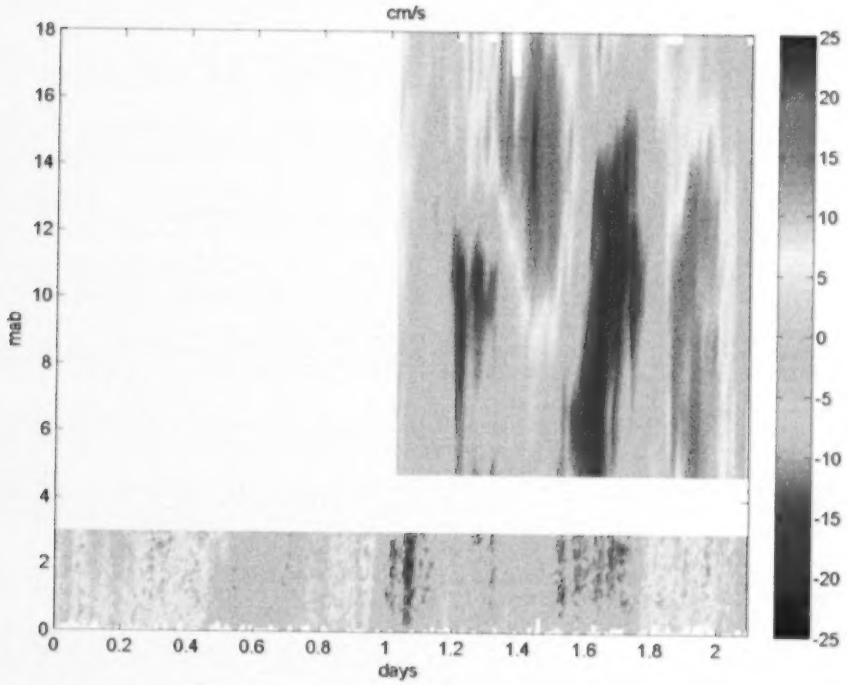

Figure 7 North component of velocity from RDI's 66_1 and 67_1

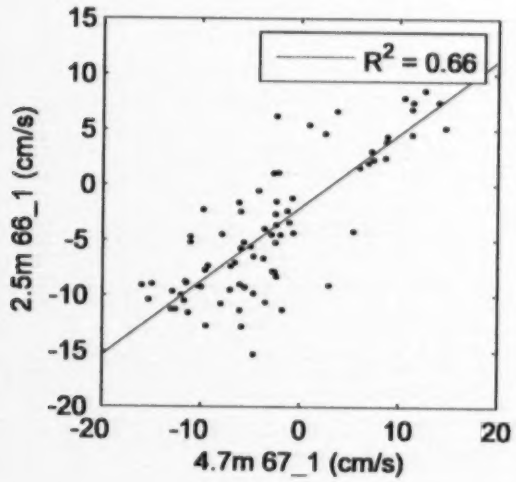

Figure 8 Regression analysis between north component of velocity from RDI's 66_1 and 67_1. Average of bins 21 to 31 (2 to 3 mab) from 66_1 was used to reduce noise.

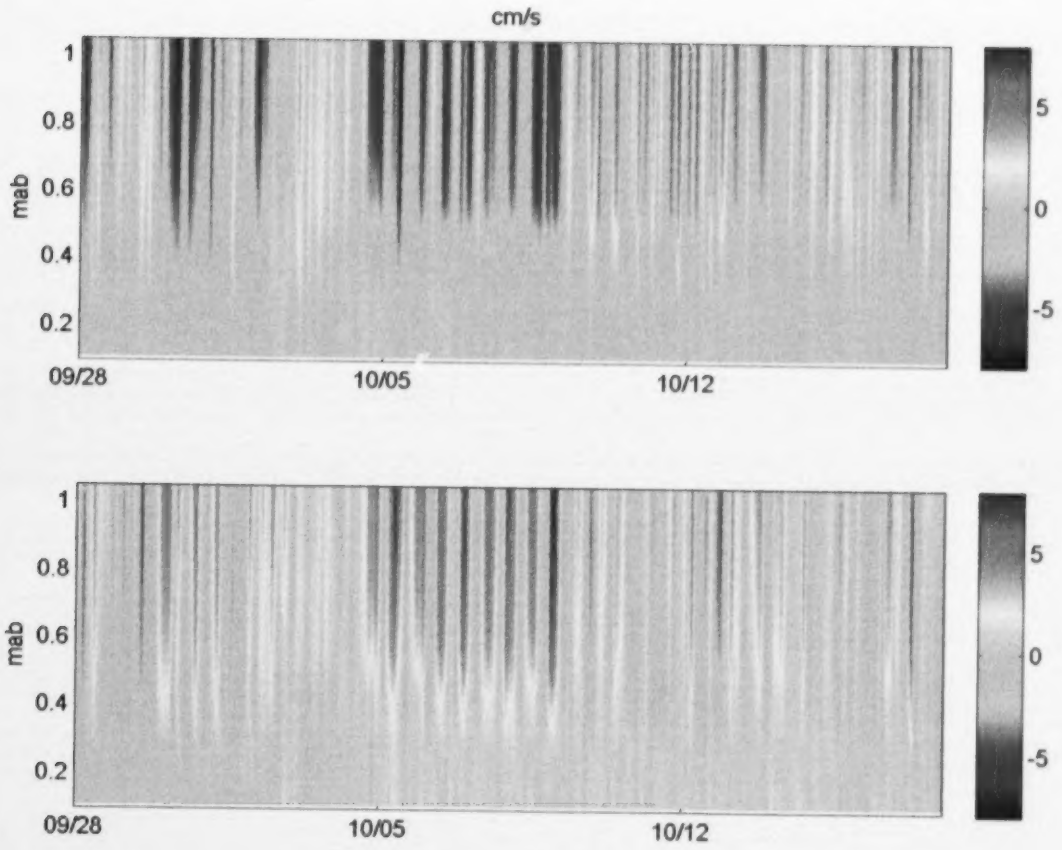

Figure 9 Aquadopp east (top) and north (bottom) velocity profile. Time axis format is MM/DD.

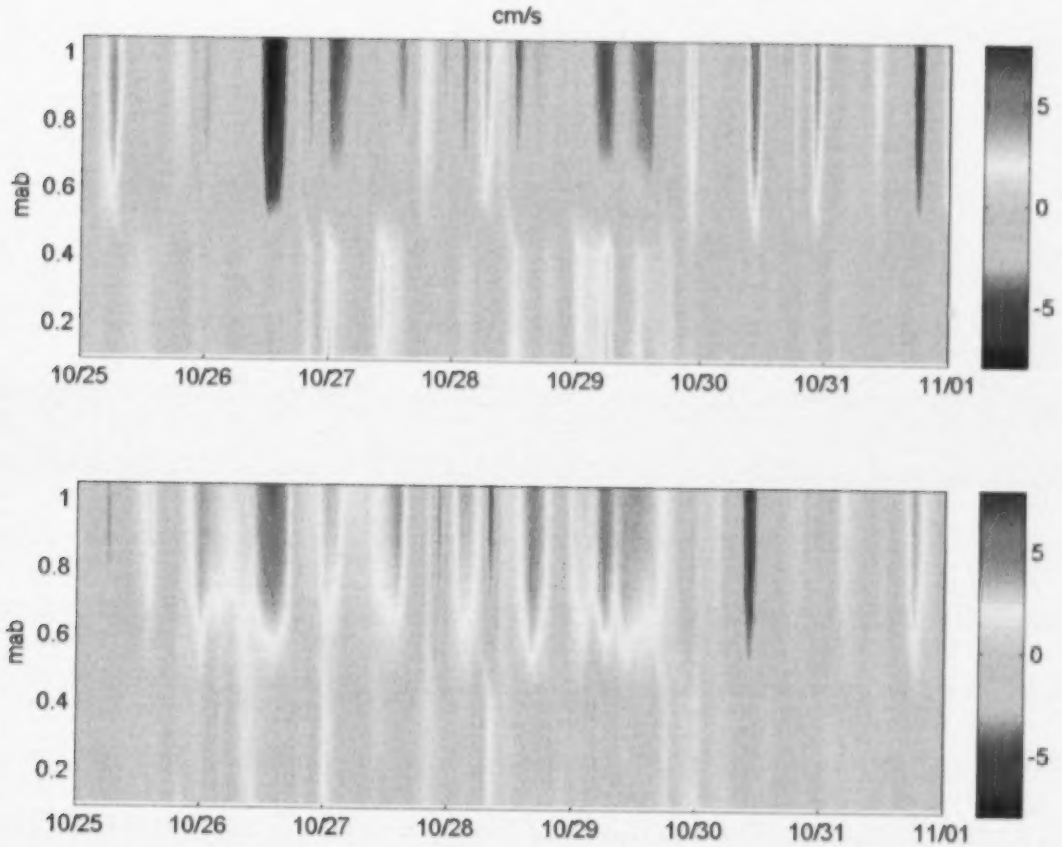

Figure 10 Aquadopp east (top) and north (bottom) velocity profile (Part 2).

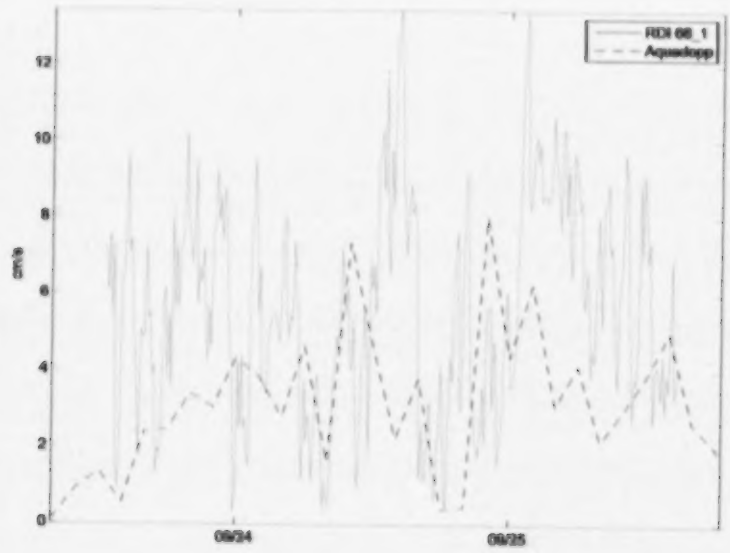

Figure 11 Speeds at 1 mab.

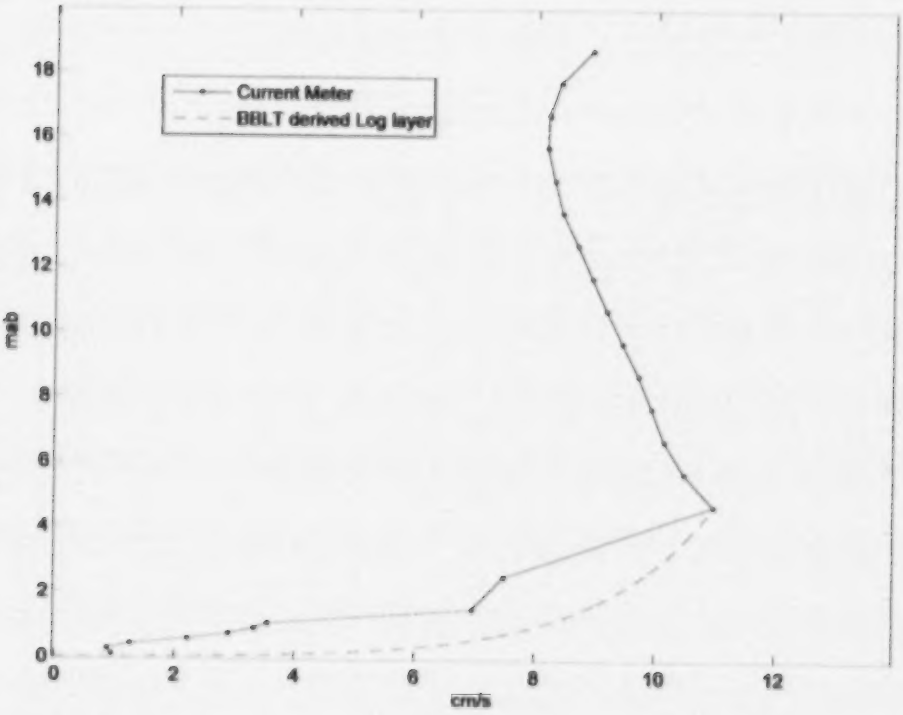

Figure 12 Root mean square velocity profile.

2.5 SIMULATIONS SETUP

Three types of forcing scenarios and 4 different sediment classes were considered, for a total of 12 simulations. The 3 forcing scenarios were (1) Full, (2) Log-layer and (3) Lin-layer (see Table 3). The 3 forcing scenarios all used the 67_1 RDI data and differ in choice of bottom and current and stress. Bottom stress in the 2 alternative forcing scenarios (2 and 3) was computed using the quadratic drag law and no wave effects.

Table 3 Forcing scenarios used in simulations.

Forcing Scenarios	NAME	Currents below 4.7 mab	Bottom stress
1	Full	66_1 and Aquadopp	Aquadopp (waves + currents)
2	Log-layer	Logarithmic bottom layer (see section 2.4)	Quadratic drag law.
3	Lin-layer	Linear bottom layer	Quadratic drag law.

The four sediment classes were, background fines, flocs, fish fecal waste, and uneaten feed pellets (See Table 4). BBLT accepts a single settling velocity and critical stress for each sediment class. Each class modelled here, was represent by average particle diameter and corresponding settling velocity and critical stress based on Law et al. (2014). In BBLT, when the bottom stress is below the critical stress, all the sediment resides on the bottom and experiences no motion until the bottom stress is exceeded.

Bottom roughness was set to 1.0 mm based on grain size analysis (=5 x grain size of 200 um). An additional modelling consideration involves the reference height (href) which is the bottom for the Rouse profile in BBLT and can be different from the roughness height as particles have finite size hence their center of mass can be above the roughness height when they are on the bottom. This is particularly important for large grains such as large fish pellets, whose average diameter is 10mm. Being higher in the water column provides exposure to stronger currents (e.g. if the speed is 1mm/s at 2 mm, it is only 0.2 mm/s at 1.1 mm for the Log-layer and 0.1 mm/s for the Lin-layer). For fines and flocs, the diameter is negligible the reference height equals the roughness height.

Table 4 Waste Class Parameters used in simulations.

Sediment Waste Class	Fines (1)	Flocs (2)	Fecal (3)	Pellets (4)
Settling velocity (mm/s)	0.1	1	40	100
Critical Stress (m/s); i.e. friction velocity)	0.003	0.003	0.009	0.015
Average Diameter (mm)	-	-	0.5	10
Reference Height (href; mm)	1	1	1.25	5
Input Mass (M_0; g)	20000	20000	20000	20000
Input Period (T; days)	1	1	1	1
Maximum Initial Concentration (C_{max}; g/m^3)	102	102	102	102

For each simulation, a mass of waste equalling M_0 grams was dumped all at once into the fish cage every T days for the entire simulation. This mass gives a maximum initial concentration of C_{max} which would only occur if all the material dumped on the first day settled in the bottom 10 cm directly under the fish cage with D (=50 meter) diameter (a volume of $Vo = 0.1\ \pi\ D^2/4 = 196.3\ m^3$ here) . Most concentrations presented in this report are normalized by C_{max} and hence can be generalized to any dumping rate and cage size simply by multiplying by $C_{max} = M_0/Vo$. The actual decent of sediment to the bottom is not modeled by BBLT. All sediment input is immediately redistributed vertically based on the Rouse profile. Hence for lighter sediment classes C_{max} is rarely achieved. The normalized concentration can exceed 1 if the sediment accumulates from daily inputs.

The original BBLT version 7.0 released all its sediment at one point, the origin. For the present work, in order to avoid anomalously large concentrations immediately after a release (as well as represent the fish cage in a more realistic fashion) a slight modification

was made to the code to release sediment over the circular area of the cage. Particles are released at random places inside the cage to more realistically represent the addition of waste components.

The simulations ran for 46 days which cover the period when data from both the aquadopp and 67_1 was available. For the purpose of the simulation, all input data time series were interpolated to a common time step of 18 minutes. These and other simulations parameters are listed in Table 5. BBLT limits the vertical extent of the resuspension with the parameter hmax. This was set to 18 m, the depth of the shallowest of the 3 instruments.

Table 5 BBLT Simulation Parameters

Start Time	Day 0 (=00:00Z 25-Sep-2014)
Duration	46 days
Number of Particles	10000 added every 24h Total =480 000
Advection time step	0.03 hours
Bottom Roughness	1.0 mm
Maximum Vertical Extent (hmax)	18 m

3: RESULTS

BBLT simulation results are presented graphically in 3 formats: time series of concentration directly below the cage (averaged over the area of the 50 m diameter cage), horizontal distribution of mean bottom concentration in the near (few 100's of meters) field and in the far (few 1000's of meters) field. Unless otherwise specified, all bottom concentrations refer to bottom 10 cm average and are normalized (see 2.5) and hence units are omitted.

3.1 FULL FORCING SIMULATION

Time series of bottom concentration below the cage is shown in Figure 13. The fines and flocs disperse rapidly in most cases leaving a near zero concentration most of the time. Fecal waste begins to accumulate over days 0 to 7 peaking at 8 (recall in the normalized units 8 means all the sediment dumped over the 8 days accumulates on the bottom inside the perimeter of the cage). The arrival of wave event E1 (see 2.2) clears the backlog and no further buildup occurs. For the feed pellets the trend is somewhat different. The early buildup occurs and clears just as for fecal waste but reappears again for days 11-22 and somewhat for days 40-45. The buildup finally clears by wave event 4 towards the end of the simulation. For fecal and feed waste, outside of the large build ups the concentrations hover between near 0 and 1 indicating adequate removal of waste.

The time series of concentration at 1 mab under the cage is shown in Figure 14. Fines and floc series are almost identical to the bottom while fecal and pellet waste is zero aside from a small spike on day 39 (Nov. 3; wave event 4).

Figure 15 shows the spatial distribution of mean (over the simulation period) concentration. There is a wide range of concentrations for the various materials. However, peak values are typically inside the perimeter of the cage and except for the fines, rapidly decrease outside. The fines have a near uniform scatter of material at very low concentrations (3-6 e-6) in the proximity of the cage with slightly higher values inside the perimeter of the cage. More informative is the far field plot which shows the range of impact of the fines (taken as e-folding distance; i.e. distance for concentration to drop to 1/e of peak value) to extend about 1.5 km North/South and 0.4 km East/West. This elliptical pattern is consistent with the M2 tidal ellipse although major to minor ratio is about double at 4:1. Tidal excursion (calculated by taking the half the M2 major axis amplitude over half the tidal period) gives about 800 m. Hence the elliptical pattern is attributed to the back and forth motion of the tides.

The flocs also disperse leaving a small residual mean concentration of 6e-4 inside the cage. e-folding length is reached just outside the cage indicating this class spends more time near the bottom and hence does not move as freely with the tide as the fines.

Mean fecal and pellet waste concentrations are 1.2 and 2.7 and almost zero outside the cage diameter, although fecal waste extends ~80m northwest of the cage. The far field plots show that the waste never reaches outside of an ellipse 1000 m North/South and 0.5 km East/West (i.e. white indicates zero particle count) during the simulation period.

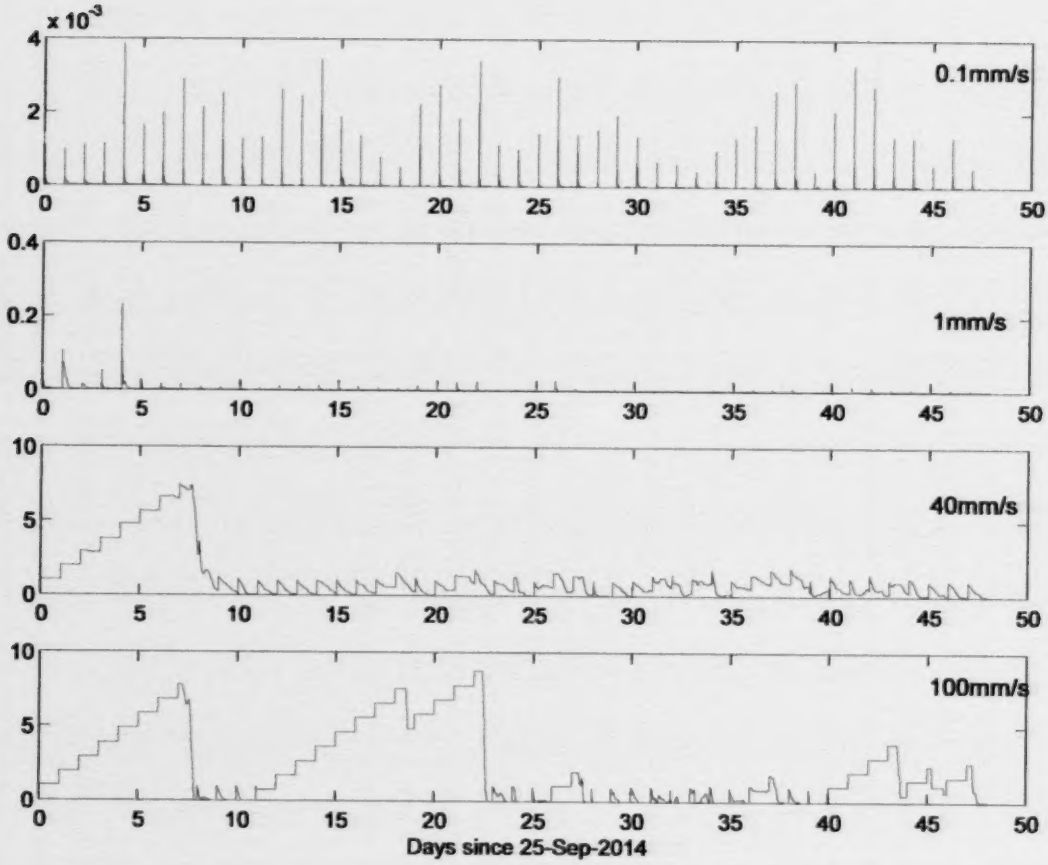

Figure 13 Normalized bottom concentration under fish cage for the 4 sediment classes forced with the Full forcing scenario.

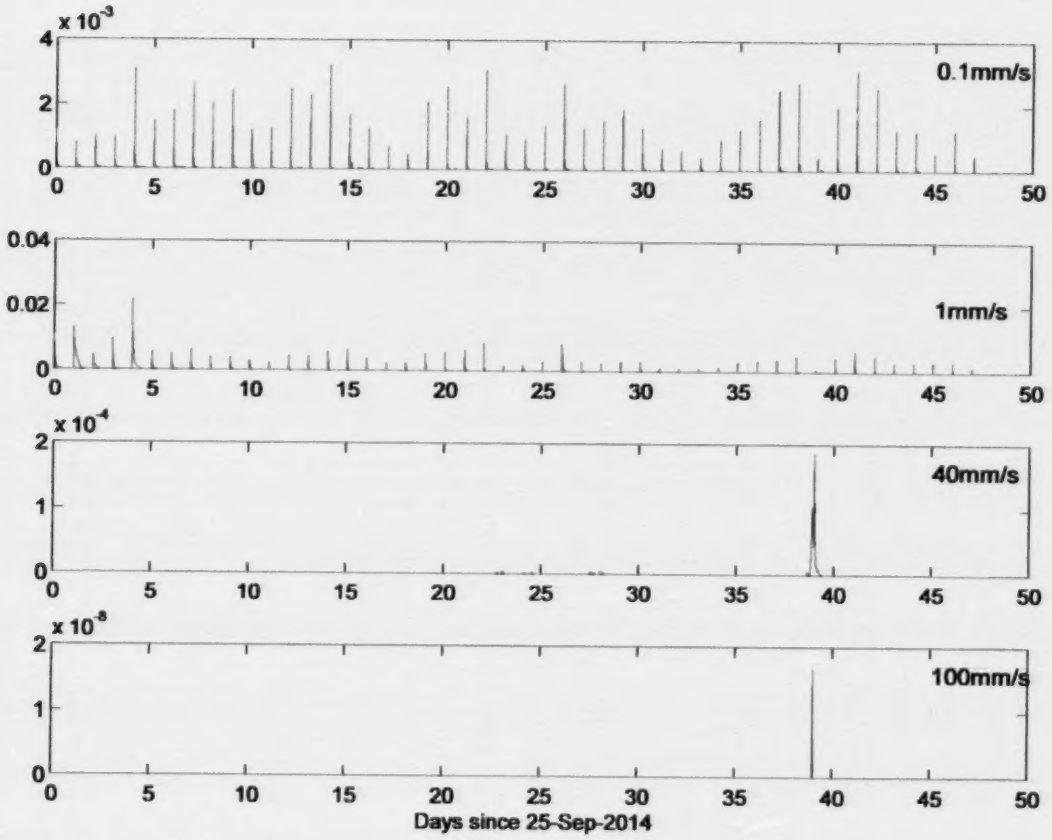

Figure 14 Normalized concentration 1 meter above bottom under fish cage for the 4 sediment classes forced with the Full forcing scenario.

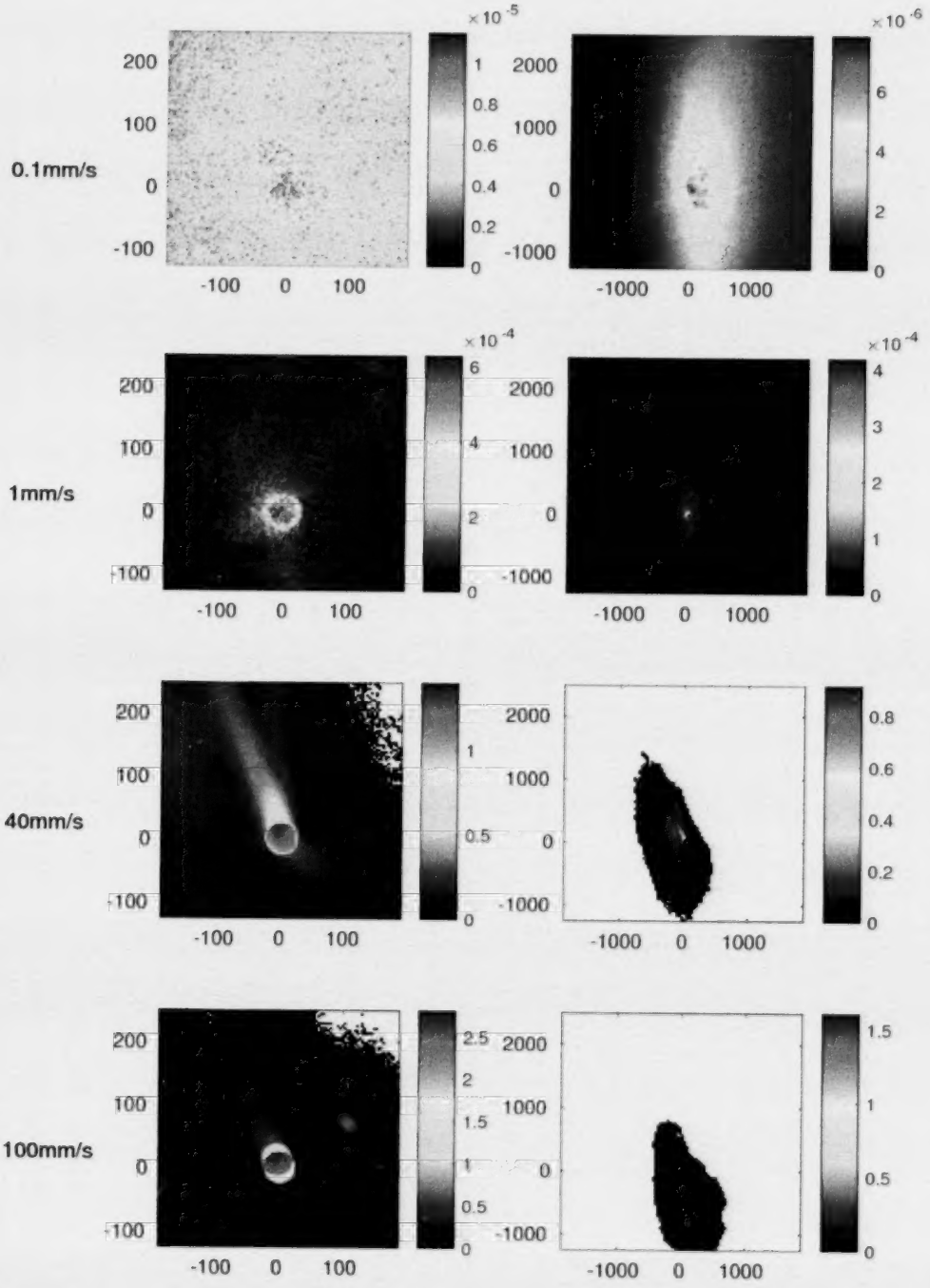

Figure 15 Near field (left) and far field (right) normalized mean bottom concentration for 4 waste class scenarios for the Full forcing simulation. Horizontal units are meters in all spatial distribution plots.

3.2 ALTERNATIVE FORCING SIMULATIONS

Time series of concentration at the fish cage for the Log-layer scenarios are shown in Figure 16. The fines and flocs disperse rapidly with occasional spikes extending to 1. This indicates low bottom stress periods where all sediment recently added temporarily settles to the bottom and then is rapidly removed when bottom stress increases. Fecal waste tends not to accumulate with typically all the material removed before addition of new material in 24 hours. There are a few exceptions where the concentration reaches 2 before dispersing. Pellets time series has a saw tooth shape with cycles of buildup and dispersal peaking around 10.

The spatial distribution of mean concentration is shown in Figure 17. For flocs and fines, the concentrations are about 2 orders of magnitude higher than in the full scenarios and do not peak inside the cage. This is indicative of a very mobile sediment cloud, which occasionally impacts the bottom during low stress events. For the fecal and pellet waste, the concentration is high in proximity of the cage with stronger dispersal along the North-South axis. Episodic deposition time history can be seen as 50 m (cage sized) circles of increased concentration for the pellets. Evidently when the pellets became mobile, they migrate to a new location (without significant dispersion) and became deposited there for some time before migrating again.

For the Lin-layer scenario (Figure 18 and 19), the fines and flocs behave much like the Log-layer case, albeit with more frequent spikes which is consistent with the lower bottom currents with this forcing scenario. The lower currents become more evident in the fecal and floc cases where the sediment is unable to clear the cages and continues to build up during the simulation.

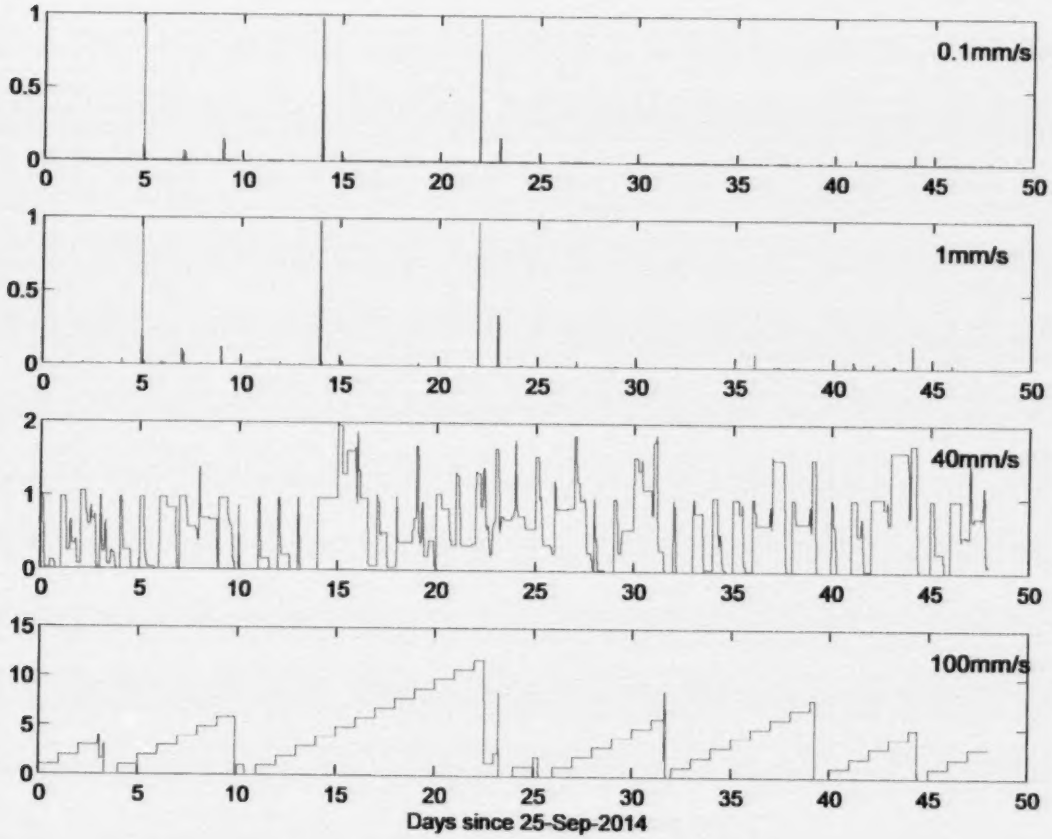

Figure 16 Normalized bottom concentration under fish cage for the 4 sediment classes forced with the Log-layer forcing scenario.

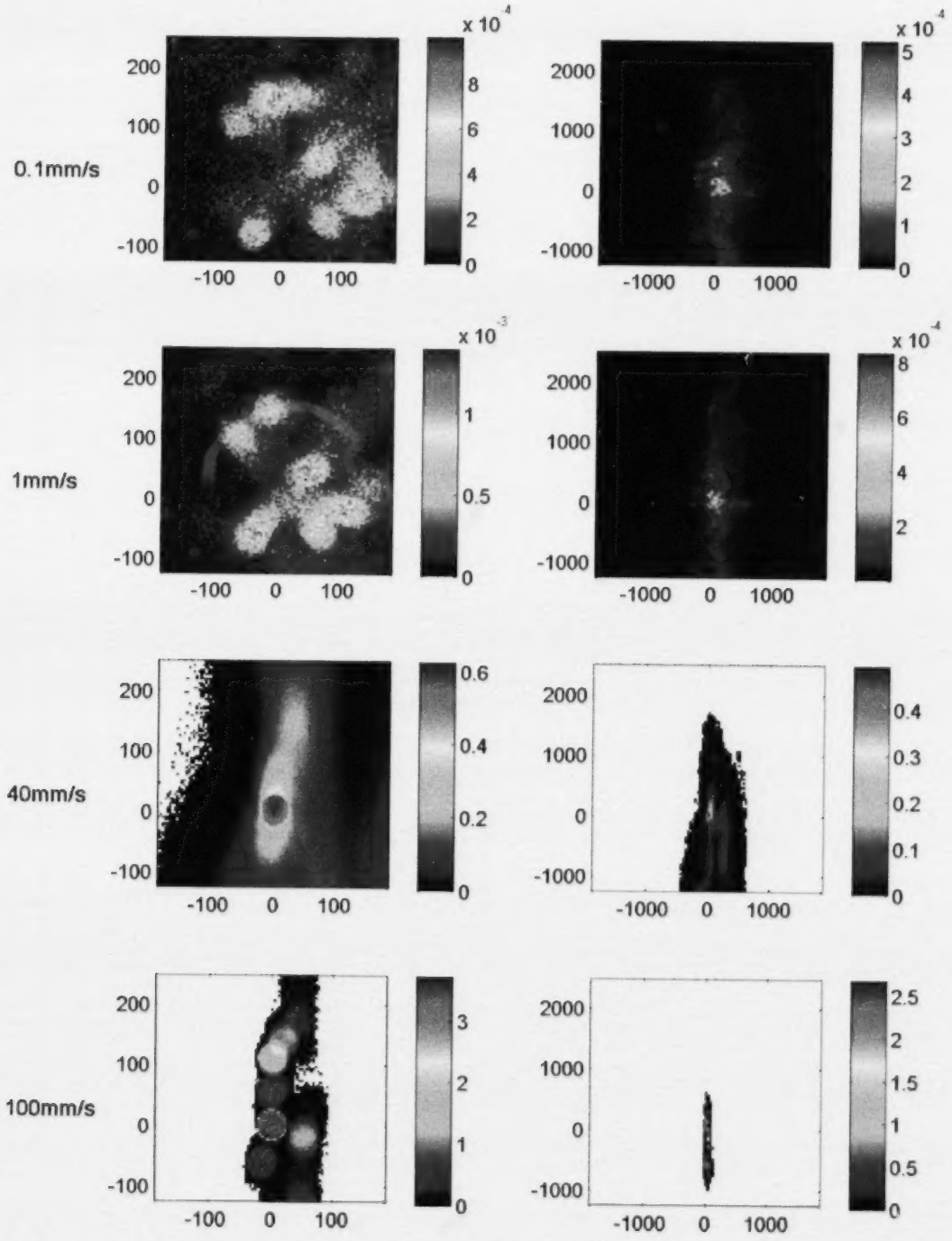

Figure 17 Near field (left) and far field (right) normalized mean bottom concentration for 4 waste class scenarios for the Log-layer forcing simulation. Horizontal units are meters in all spatial distribution plots.

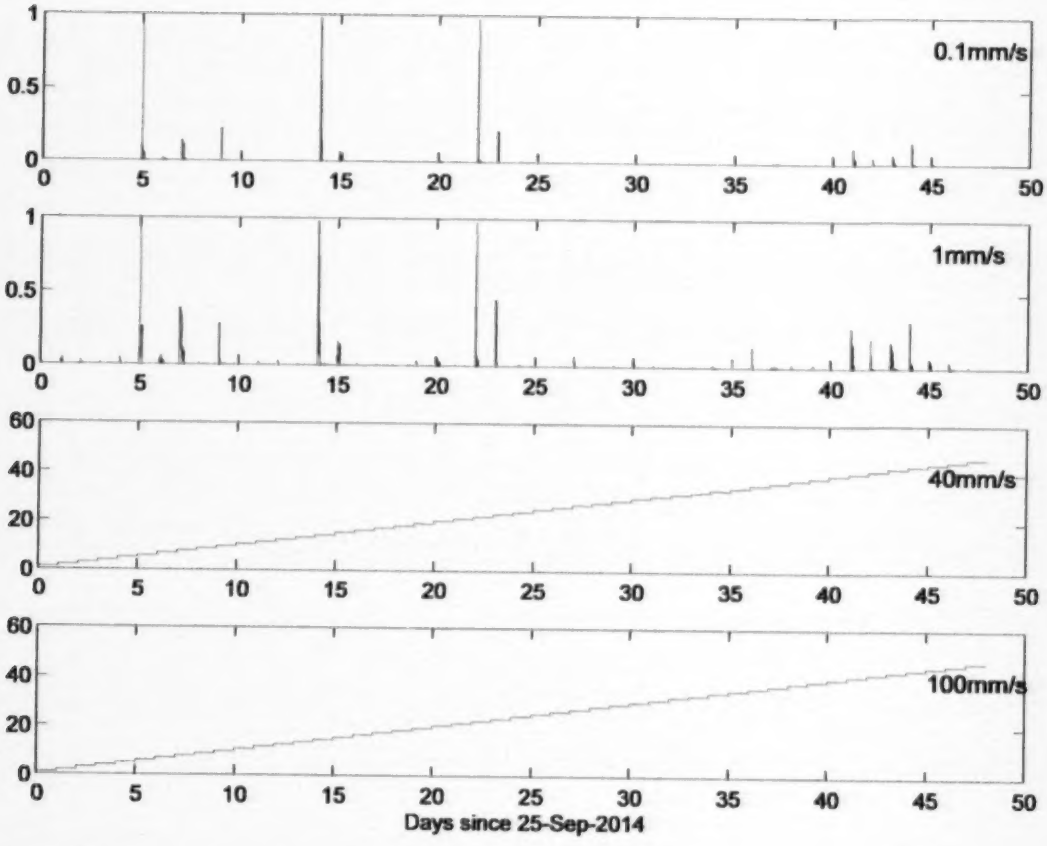

Figure 18 Normalized bottom concentration under fish cage for the 4 sediment classes forced with the Lin-layer forcing scenario.

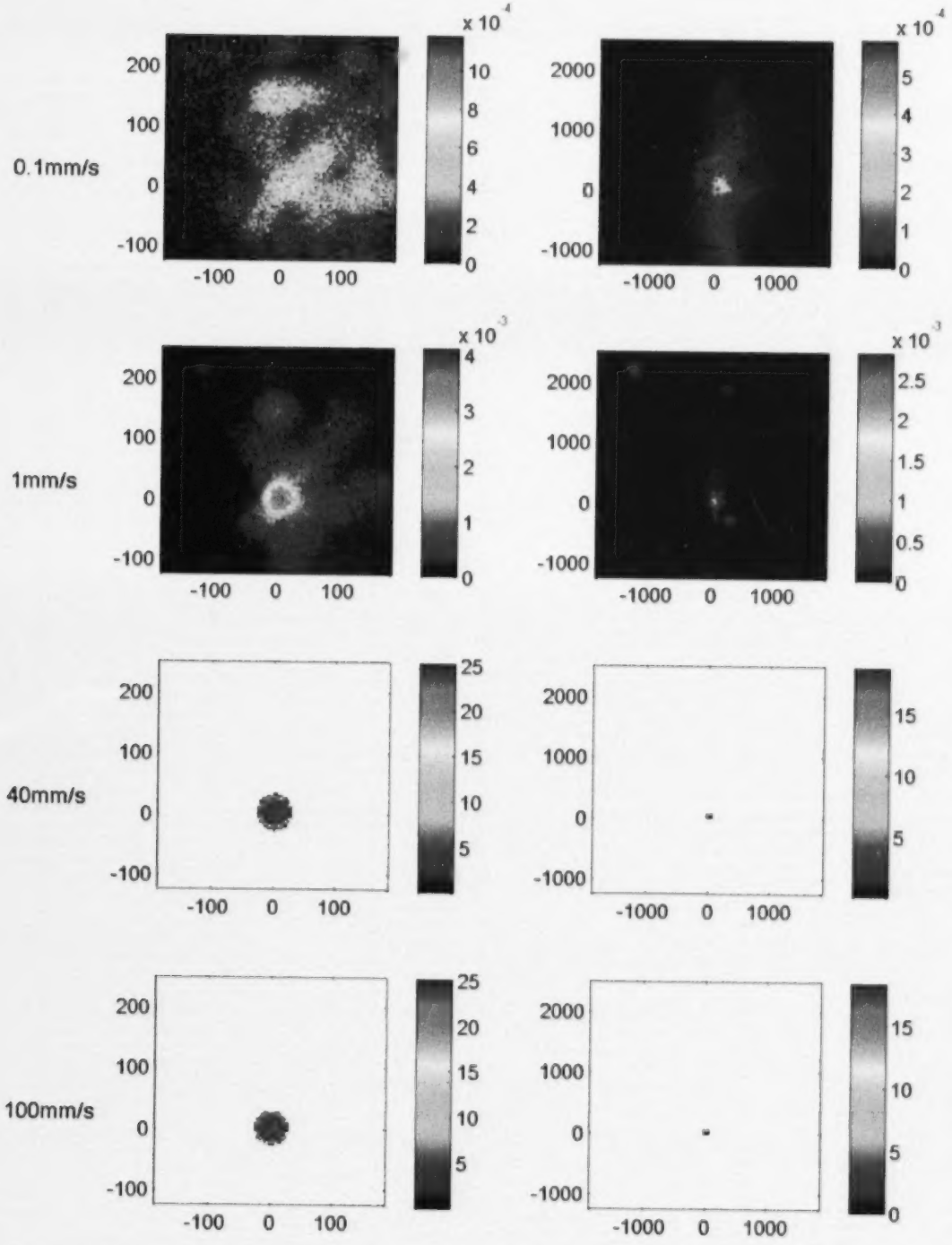

Figure 19 Near field (left) and far field (right) normalized mean bottom concentration for 4 waste class scenarios for the Lin-layer forcing simulation. Horizontal units are meters in all spatial distribution plots.

4: DISCUSSION

The fate of fish cage waste was investigated using the BBLT model. Four settling velocities representing different sedimentary waste classes were considered with a discharge scenario of one bulk input per day. The discharge scenario can be summarized by the equation:

$$\frac{dC}{dt} = -\frac{C}{\propto} + \frac{C_{max}}{T} \qquad \text{Eq. 1}$$

where C is the concentration and $\propto$ is the e-folding period. The steady state solution to Eq. 1 is

$$\frac{\propto}{T} = \frac{C_0}{C_{max}} \qquad \text{Eq. 2}$$

where C_0 is the equilibrium concentration which is taken here as the mean of concentration in the bottom 10cm under the cage as presented in the time series in Chapter 3. In some cases a steady state was not reached during the 46 day run (as required by Eq. 2). The results are summarized in Table. As can be seen, C_0 varies by up to 6 orders of magnitude between the 4 different waste categories and 3 forcing scenarios.

Table 6 Summary of Results. Normalized concentrations and e-folding periods are equal (See Eq. 2 and Section 2.5) hence are listed in same column. Values proceeded by >, indicate that steady state was no reached. Heights are the Mean/Maximum of the center of mass of all sediment.

Settling Velocity (mm/s)	C_0 / C_{max} (normalized) or $\propto$/T	C_0 (g/m^3)	Mean/Maximum Height Above Bottom (meters)	Mean/Maximum Rouse Number	Percentage of time in deposition
Full forcing scenario					
0.1	3 e-5	0.003	8.9 / 9.0	1.5e-2 / 3.5 e-2	0
1	8 e-4	0.082	7.2 / 8.5	0.15 / 0.35	0
40	1.2	122.4	1.8e-3 / 6.5e-3	5.9 / 14	15
100	2.3	234.6	5.3e-3 / 7.0e-3	14.8 / 34.9	62
Log-layer scenario					

0.1	2 .0-3	0.204	8.1/9.0	4.5e-2/0.7	8
1	2.6e-3	0.265	6.2/8.4	0.5/6.5	8
40	0.6	61.2	1.3e-3/1.7e-3	18.5/261	75
100	3.5	357.0	5.0e-3/5.6e-3	46.2/653	99.1
Lin-layer scenario					
0.1	2.5e-3	0.255	8.1/9.0	4.5e-2/0.7	8
1	5.9e-3	0.602	6.2/8.4	0.5/6.5	8
40	>47	>4794	1.3e-3/1.7e-3	18.5/261	75
100	>47	>4794	5.0e-3/5.6e-3	46.2/653	99.1

The alternative scenarios demonstrate the importance of resolving the bottom of the water column and the crucial role that the waves play at this location. For both the Log-layer and Lin-layer forcing scenarios, the lack of wave induced bottom stress manifests itself in higher concentrations. For fines and flocs, the difference is about 2 orders of magnitude. This large difference can only be explained by deposition since the mean vertical height for all 3 forcing scenarios is in the 6 to 9 meter range (Table 6; column 4). In the Full forcing scenario, the bottom stress never goes below the critical stress while for the alternative scenarios 8% of the time is spent in deposition (Table 6; column 6).

For the fecal and pellet waste, the loss of wave induced bottom stress in the alternative scenarios leads to significantly more time in deposition, 99 % compared to 62 % in the Full forcing scenario. The impact of this additional time in the deposition is higher concentration, as the sediment piles up without much dispersal. However, in the Log-layer case, the higher bottom currents partially compensate for the lack of waves. The 1% of suspension time is adequate to periodically clear the buildup and only lead to mean concentrations that are about 50% higher the full simulation in the case of the pellets (In the case of the fecal waste, the Log-layer concentrations are actually lower than the Full). The situation is very different for the Lin-layer case where both the heavy settling categories continue to pile up without a steady state (Eq. 2) being reached during the 46 day simulation.

These 2 alternative forcing scenarios were chosen because they represent the range of options for extrapolating near-bottom currents in the absence of data. As was shown the Log-layer overestimates while the Lin-layer underestimates the near bottom currents. At the present site, the Log-layer is a much better alternative than the Lin-layer even though the rms profile (Figure 12) suggest otherwise. Evidently what matters for the fecal and pellet waste is in the 10 cm near bottom as that's where this waste spends most of its

time. This comparison underlines the importance of accurate near-bottom currents and bottom stress as provided by the aquadopp in this investigation.

The results show that the sediment transport process is highly sensitive to the choice of extrapolation of near bottom currents, critical stress, and the BBLT parameter: bottom reference height (href). This sensitivity becomes critically important for heavier particles which are limited to a few millimeters off the bottom. Figure 20 demonstrates this with 4 choices of bottom parameterization for the Full forcing pellet scenario. In the top panel href=1mm (i.e. the large particle is assumed to be a point) and the currents below the lowest aquadopp bin (10 cm) are extrapolated linearly to the bottom (=0 at 1mm). The concentration inside the cage continues to build with little or no clearance much as for the Lin-layer case above. Moving from linear to log (panel 2) brings the concentration down to reasonable values. The third panel shows the effect of increasing href to 5mm as used in the Full simulation. The concentration decreases further and resembles the fecal waste in the Full scenario. The last panel shows the concentration with the actual Full scenario parameters used here, which in addition to the features of panel 3 has the deposition module turned on.

In light of the high level of sensitivity to the bottom parameterization, the results presented here should be interpreted cautiously until validation and tuning with field data is possible. Direct model validation with *in-situ* concentrations poses a challenge due to knowledge gaps such as actual fish cage waste amounts and background concentrations. However, the spatial structure of the concentrations offers a possible means for validation by comparing the relative concentration at various locations around and inside the cage. This can best illustrated by looking at the spatial distribution of the concentration on a logarithmic scale (Figure 21) which highlights the background concentrations around the cage. The ratio between the sediment samples taken inside the cage and those outside can be compared directly with this figure. For fines, the ratio should be close to 1 and relatively uniform within a few hundred meters of and inside the cage. Samples would need to be taken a few kilometers for concentrations to fall by an order of magnitude. Flocs ratio should fall to 1/10 within a 100 m of the cage and to 1/1000 within a few kilometers. For fecal waste, the ratio is 1/10 directly outside the cage and should be undetectable (i.e < 1e-6) within a kilometer (faster along East-west axis, particularly eastward). For pellets the situation is somewhat more complicated due to the episodic deposition and advection of the sediment patch which appear as cage sized features with increased concentration. The dispersion process is very slow for this waste and the time history matters (i.e. this picture is likely to be quite different if this experiment was repeated at different points in time). However, we can still conclude that like for the fecal waste the concentration ratio drops by at least an order of magnitude directly outside the cage and by as much as 1/1000 within a few hundred meters. The general direction of travel is to the south.

The results presented here are based on physics alone. With organic waste, the chemical and biological processes are a significant factor. In particular, for the long e-folding times of feed pellets, decomposition and opportunistic feeding by wild species should not be neglected. Nevertheless, the values in Table 4 provide an upper limit.

Implications for contaminant/pesticide transport

Results of this study suggest that fines and flocs can be transported to the far-field (i.e. km's from the site). The concentration of these materials does decrease but also provide a mechanism for organics, contaminants, other chemicals (e.g. pesticides) that are particle reactive to be transported. It is a recommendation of this study to continue to validate these findings and use models to increase our predictive capacity of aquaculture operations.

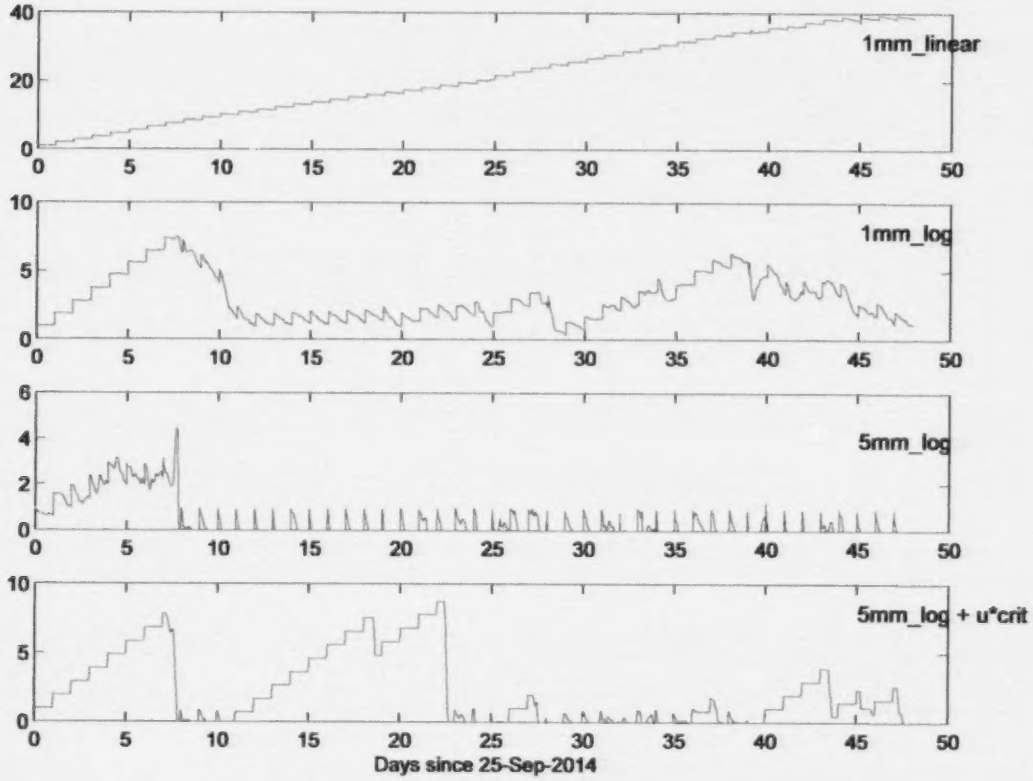

Figure 20 Normalized bottom concentration under fish cage forced with the Full scenario for feed pellets. Panels from top to bottom test the sensitivity of the bottom parameterization (see Discussion).

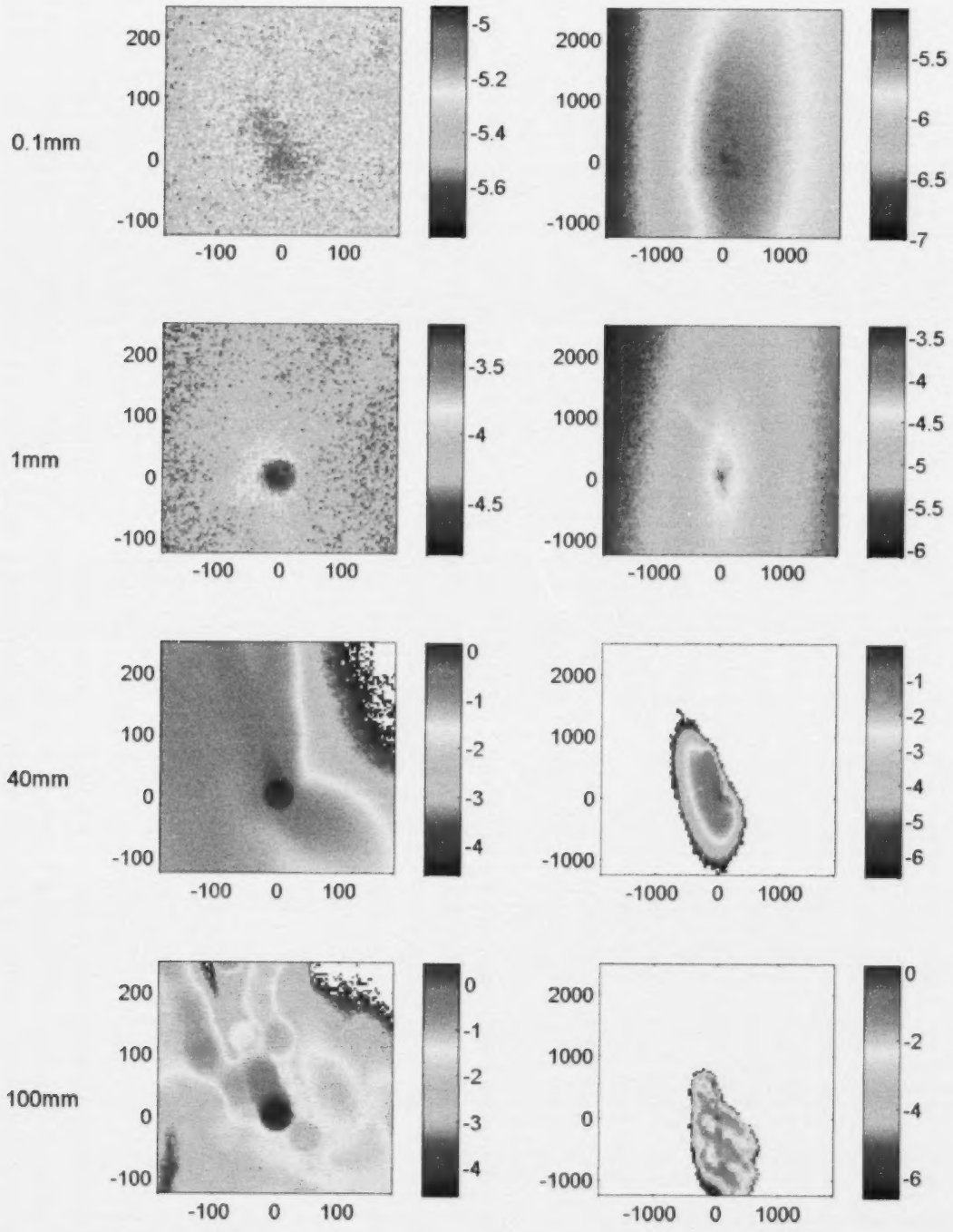

Figure 21 Near field (left) and far field (right) normalized mean bottom concentration for 4 waste class scenarios for the Full forcing simulation (base 10 logarithmic color scale). Horizontal units are meters in all spatial distribution plots

ACKNOWLEDGMENTS

We would like to thank Vanessa Zions, Casey O'Laughlin, Sarah Scouten and Randy Losier and the crew of the CCGS Viola Davidson for excellent filed support. Much gratitude is due to Dr. Yongsheng Wu and Sebastien Donnet for their helpful review of this document. Funding was supplied by PARR, the Program for Aquaculture Regulatory Research.

REFERENCES

AMEC E&E Division, 2007. Physical oceanography input to the effluent modelling study for the long harbour commercial processing plant environment assessment. oceanographic component: Effluent solid waste dispersion modelling, short and long term fate. Report prepared for Voisey Bay Nickel Ltd.

AMEC E&E Division, 2011. Labrador – Island Transmission Link. Strait of Belle Isle: Oceanographic Environment and Sediment Modelling. Report prepared for Nalcor Energy Ltd.

Csanady, G.T. 1982. Circulation in the coastal ocean. Reidel, London

Cranford, P. J., Gordon, Jr., D. C., Hannah, C. G., Loder, J. W., Milligan, T. G., Muschenheim, D. K., Shen, Y., 2003. Modelling potential effects of petroleum exploration drilling on northeastern Georges Bank scallop stocks. Ecological Modelling 166,19-39.

Drozdowski, A., Hannah, C., Tedford., T., 2004. BBLT Version 7.0 user's manual. Can. Tech. Rep. Hydrogr. Ocean Sci. 240: vi + 69 pp. Available from www.mar.dfo-mpo.gc.ca/science/ocean/coastal_hydrodynamics/WEBBBLTgui/BBLTgui.html

Drozdowski, A. 2009. BBLT3D, the 3D Generalized Bottom Boundary Layer Transport Model: Formulation and Preliminary Applications . Can. Tech. Rep. Hydrogr. Ocean Sci. 263: vi + 32 pp.

Grant, W. D., Madsen, O. S., 1986. The continental shelf bottom boundary layer. Annual Review of Fluid Mechanics 18, 265-305.

Haibo, N., Drozdowski, A., Lee, K., Veitch, B., Reed, M., Rye, H., 2014. Modeling the transport of drilling muds: comparison of BBLT and ParTrack models. Oceans - St. John's, 2014. IEEE. DOI: 10.1109/OCEANS.2014.7003015

Hannah, C. G., Drozdowski, A., Loder, J. W., Muschenheim, K., Milligan, T., 2006. An assessment model for the fate and environmental effects of offshore drilling mud discharges. Estuarine, Coastal and Shelf Science 70, 577-588.

Hannah, C. G., Drozdowski, A., 2005. Characterization of drift and dispersion of drilling mud on three offshore banks. Marine Pollution Bulletin 50, 1433-1443.

Hannah, C. G., Drozdowski, A., Muschenheim, D. K., Loder, J., Belford, S., MacNeil, M., 2003. Evaluation of drilling mud dispersion models at SOFI Tier I sites: Part 1 North Triumph, Fall 1999. Can. Tech. Rep. Hydrogr. Ocean Sci. 232: v+51 pp.

Hannah, C. G., Shen, Y., Loder, J. W., Muschenheim, D. K., 1995. BBLT: Formulation and exploratory applications of a benthic boundary layer transport model. Can. Tech. Rep. Hydrogr. Ocean Sci. 166: vi + 52 pp.

Law, B.A, Hill, P.S., Maier, I., Milligan, T.G., Page, F, 2014. Size, settling velocity and density of small suspended particles at an active salmon aquaculture site. Aquaculture Environment Interactions, 6: 29-42, doi:10.3354/aei00116.

Li, M. Z., Amos, C. L., 2001. SEDTRANS96: The upgraded and better calibrated sediment-transport model for continental shelves. Comput. Geosci. 27, 619-645.

Page, F.H., Chang, B.D., Haigh, S.P., and Losier, R.J. 2016. Oceanographic observations in coastal waters of Shelburne County, Nova Scotia, 2008-2014. Can. Tech. Rep. Fish. Aquat. Sci. 3xxx: iv + 90 p.

Petrie, B., Bugden, G., Tedford, T., Geshelin, Y., Hannah, C., 2004. Review of the physical oceanography of Sydney Harbour. Can. Tech. Rep. Hydrogr. Ocean Sci. 215: vii + 43 pp.

Rouse, H., 1937. Modern concepts of the mechanics of turbulence. Trans. Am. Soc. Civ. Eng. 102, 463-543.

Rye, H., Reed, M., Frost, T. K., Utvik, T. I. R., 1998. Comparison of the ParTrack mud/cuttings release model with field data based on use of synthetic-based drilling fluids. Environmental Modelling & Software 21, 190-203.

Tedford, T., Drozdowski, A., Hannah, C. G., 2003. Suspended sediment drift and dispersion at Hibernia. Can. Tech. Rep. Hydrogr. Ocean Sci. 227: vi + 57 pp.

Tedford, T., Hannah, C. G., Milligan, T. G., Loder, J. W., Muschenheim, D., 2002. Flocculation and the fate of drill mud discharges. In: Spaulding, M. L. (Ed.), Estuarine and Coastal Modelling: Proceedings of the 7th International Conference. ASCE, pp. 294-309.

Teledyne RD Instruments (2014). WorkHorse Sentinel, Monitor, and Mariner Operation Manual. Teledyne RD Instruments, Poway, CA, USA.